Leaching of Electric Arc Furnace Slag for Selective Recovery of Iron: Effect of Temperature, H_2SO_4/HCl Acid, and Oxidant Concentration

Faizatul Syazwani Zulkifili[1], Hawaiah Imam Maarof[1,2], Norhaslinda Nasuha[1,2] and Siti Wahidah Puasa[1,3]*

[1]*School of Chemical Engineering, College of Engineering, Universiti Teknologi MARA, 40450 UiTM, Shah Alam, Selangor, Malaysia*
[2]*Hybrid Nanomaterials, Interfaces & Simulation (HYMFAST), School of Chemical Engineering, College of Engineering, Universiti Teknologi MARA, Cawangan Pulau Pinang, 13500 UiTM, Permatang Pauh, Pulau Pinang, Malaysia*
[3]*Integration Separation Technology Research Group (i-STRonG), College of Engineering, Universiti Teknologi MARA, 40450 UiTM, Shah Alam, Selangor, Malaysia*

ABSTRACT

A significant amount of electric arc furnace slag (EAFS) is generated as a by-product from the steelmaking industry. Acid leaching was carried out with both the presence and absence of oxidants to intensify the iron recovery from EAFS in the final product. Oxidative leaching refers to the process whereby the oxidant helps in removing one or more electrons in a chemical reaction. In contrast, non-oxidative leaching means there is no transfer of electrons during the process. In this study, hydrogen peroxide and potassium permanganate were used as the oxidants in the leaching process. The influences of the leaching factors, such as the concentration of leaching reagent (0.5–8 M), leaching temperature (323–363 K), EAFS particle size (50–300 µm) and concentration of the oxidants (0.5–2 M), were also studied. The findings revealed that the particle size, acid dosage and type of oxidants significantly influenced iron recovery. Smaller particle sizes greatly improved the recovery of iron. İn the non-oxidative leaching environment, sulphuric acid exhibited a higher iron recovery than hydrochloric acid. The recovery efficiency was 21.47% higher. For oxidative leaching, the leaching efficiency of iron was more favourable at lower concentrations of hydrogen peroxide in both sulphuric and hydrochloric acid, and the

opposite was the case for potassium permanganate. An overdose of hydrogen peroxide can cause radical quenching, which will reduce oxidant utilisation. Oxidative leaching resulted in better iron recovery at optimum leaching conditions with a temperature of 50°C, 5 M H_2SO_4, 1 M hydrogen peroxide, a leaching time of 60 minutes, a solid to liquid ratio of 1:20 and a stirring rate of 300 rpm.

INTRODUCTION

Steel makes a major contribution to the development of the modern world across the globe due to its many applications in appliances, construction, and transportation (Keymanesh et al., 2021; Kim & Azimi, 2020; Zhang et al., 2019). Thus, steelmaking production is expected to be tremendous to meet the high steel demand. As reported by the World Steel Association, the production of crude steel up to March 2021 was 169.5 million tonnes with an increment of 23.3% compared to April 2020 and with China being the largest steel producer. Monosi et al. (2016) reported that the discharged product from crude steel production is around 11–20 kg per ton of steel. Iron slag can be categorised into several categories corresponding to their processes: blast furnace slag (BFS) and electric arc furnace slag (EAFS).

EAFS is one of the by-products of the steelmaking industry, resulting from the melting and preliminary acid refining of the liquid steel. It is typically dark in colour, angular shaped fractions and has a hard and rough texture (Hafez et al., 2021; Martinho et al., 2018; Roy et al., 2020). Teo et al. (2019), Fisher and Barron (2019), and Roy et al. (2019) previously reported that the major components of EAFS consist of iron, calcium, silica and traces of manganese and lead. Most metallurgical companies generate large amounts of hazardous wastes containing dissolved toxic metals. Landfilling or incineration are the traditional techniques for disposing of this solid waste, although neither approach appears to be effective (Kremser et al., 2021; Plaza et al., 2021). Meanwhile, the constant opening of landfills is always linked to environmental risks as this not only disrupts flora and fauna but also takes up more space. Halli et al. (2020) reported that landfilling with this metal-containing waste should not be promoted due to the toxic and carcinogenic nature of EAFS. Furthermore, dumping can also reduce the porosity and permeability of the soil (Roy et al., 2018). Currently, waste reduction takes precedence over other methods, and landfilling waste should be the final option to be considered (Yang et al., 2017).

Recycling and promoting the utilisation of EAFS has been identified as the best sustainable alternative when handling the vast amount of solid waste generated by the steelmaking sector. Brooks et al. (2019) reported that recycling helps by diverting waste from landfills, allowing it to be recovered into usable secondary products, hence conserving

energy and resources. However, preliminary research on the recycling of ferrous metals from EAFS means its application has been limited. Prior research on leaching from electric arc furnace slag has been identified. However, those findings have focused on non-ferrous metals such as zinc, phosphate and manganese recovery with no iron in the final product. Several studies have been conducted on the recycling of iron for secondary applications. Previously, Nasuha et al. (2017) discovered the usage of activated EAFS as an effective Fenton catalyst in photodegrading methylene blue and acid blue. Additionally, Nasuha et al. (2016) explored how EAFS may be used and recycled as a wastewater treatment catalyst. It was found that through a heterogeneous Fenton-like reaction, the thermally treated EAFS was capable of eliminating organic dyes. However, the work to selectively recover and maximise the amount of iron in the final product (the catalyst) has not been adequately addressed due to the complex composition of iron itself.

In the previous work, the leaching of iron from EAFS was done (Nasuha et al., 2019); however, the leaching was done at a high temperature and longer reaction time. In addition, the total dissolution of iron from EAFS using nitric acid also has not been highlighted. Given these issues, the goal of this study was to evaluate an existing leaching technique for increasing the amount of selectively iron in the final product to be used as a catalyst in a shorter period and at a lower leaching temperature. Since iron is the element that makes up approximately half of the slag composition, this was seen as an excellent way to recover iron at its maximum capacity and a lower cost. By utilising this method, raw iron utilisation can be reduced, and earth sustainability can be achieved.

METHODOLOGY

Material

The EAFS was obtained from a local steel company in Penang. Sulphuric acid (H_2SO_4, 98%), hydrogen peroxide (H_2O_2, 30%), potassium permanganate ($KMnO_4$), nitric acid (HNO_3, 70%) were purchased from Sigma-Aldrich while hydrochloric acid (HCl, 37%) was obtained from Merck. The particle size, temperature and concentration of the studied oxidant were 50-300 µm, 50–90°C and 0.5–8 M, respectively.

Method

The EAFS was crushed in a ball mill and sieved to a size range of 50–300 µm. The raw sample was sent for X-ray fluorescence (XRF) (PANanalytical, Epsilon 3-XL) to determine the minerals' composition. In determining the initial iron concentration, 0.5 g crushed EAFS was diluted in 100 mL nitric acid with a solid to liquid ratio of 1 to 200 for 120 minutes. The leachate was then sent for atomic absorption spectroscopy, AAS (Hitachi, Z-2000) for further analysis. For non-oxidative leaching, the powdered EAFS (5 g) was added into 100

mL of an acid solution of predetermined concentrations between 0.5-8 M at a solid to liquid ratio of 1:20. The mixture was heated at 50°C for 60 minutes and filtered. The filtrate was then sent for analysis using a spectrophotometer (Hach, DR6000). FerroVer iron reagent powder pillows (Hach, range: 0.02 to 3.00 mg/L) were used with the spectrophotometer (510 nm) to analyse the amount of iron in the leachate, and it was allowed to react for three minutes. Next, hydrogen peroxide was added as the oxidising agent to the leaching medium and stirred at 300 rpm for the oxidative leaching environment. Meanwhile, the hydrogen peroxide was replaced by potassium permanganate. The leaching experiments were conducted three times to achieve the average value.

RESULTS AND DISCUSSION

XRF Analysis

XRF analysis was performed to determine the chemical composition of EAFS and was tabulated in Table 1. It can be seen that Fe, Ca, Si, Al, Mg and Mn were all present in significant concentrations. Iron, calcium, and silicon oxides made up roughly around 75% of the chemical compositions with minor traces of magnesium and manganese oxides.

Size of Particles

Various particle sizes in the range of 50 to 300 μm was prepared. Nitric acid was chosen as the lixiviant in determining the initial concentration of iron in the raw EAFS as it acts as a strong oxidising agent, which renders it a competent leaching

Table 1
Chemical composition of EAFS

Oxides	%
Fe_2O_3	26.79
CaO	35.61
SiO_2	15.04
Al_2O_3	5.15
MgO	3.59
MnO	4.36

Table 2
Recovery of Fe in nitric acid solution

Size (μm)	Amount of Iron Being Leached Out (mg/L)[*]
50	1600
75	2400
125	1300
200	2000
300	1000

*Amount of iron being leached out: ± 1%

agent for EAFS (Rao et al., 2021). Furthermore, it can dissolve most metals to form metal nitrates (Mohammadzadeh et al., 2020). A solid to liquid of 1 to 200 was selected because it improved the solution's viscosity and promoted better leaching. The initial iron concentration was exactly 5000 mg/L, and the characterisation in size variation on the recovery of iron is shown in Table 2. From the Table 2, it can be seen that 75 μm resulted in the highest iron recovery with 48% recovery efficiency. Particles below 50 and 125 μm were considered fine and coarse materials, respectively. Zhang and Liu (2017) reported that the tendency for finer materials to remain near the top and coarse materials to roll down towards the base of the container might result in spatial heterogeneity in particle size. Thus,

this occurrence leads to fluctuations in the recovery of iron from particles of different sizes. The highest iron recovery from the various sizes resulted from 75 μm because this size was gradually exposed to the leaching solution, enabling more dissolution (Ji et al., 2021; Yin & Chen, 2021). Therefore, 75 m was selected as the size in the subsequent experiments.

Effect of Temperature

Temperature plays an important role in hydrometallurgy as it relates to the kinetics of the reaction (Hazaveh et al., 2020). The amounts of iron recovered from different leaching lixiviants are shown in Figure 1. It can be reported that leaching in sulphuric acid is higher than hydrochloric acid. Therefore, the optimum temperature was 50°C (at 5 M H_2SO_4) when 5966.7 mg/L of iron was leached out. Kukurugya et al. (2015) proclaimed that the highest iron reaction was 95°C with 1M H_2SO_4. However, it was contradictory to this study as the leaching agent concentration made a major difference. It was because, at low sulphuric acid concentration, the amount of sulphuric acid remained low and unable to supply sufficient SO_4^{2-}. As a result, it could not form the $Fe_2(SO4)_3$ complex. Also, the heat generated by 5 M H_2SO_4 was higher than that of 1 M H_2SO_4, and it can react at a lower leaching temperature. The drastic drop in iron concentration between 50 and 60°C in the HCl environment was because most iron has been leached out at 50°C and the remaining hard iron in the core of EAFS was still accessible to the lixiviant albeit difficult. Also, the diffusion of the lixiviant to contact the surface of this metals fraction was the rate-limiting step. Therefore, 50°C was selected as the optimum temperature for iron dissolution.
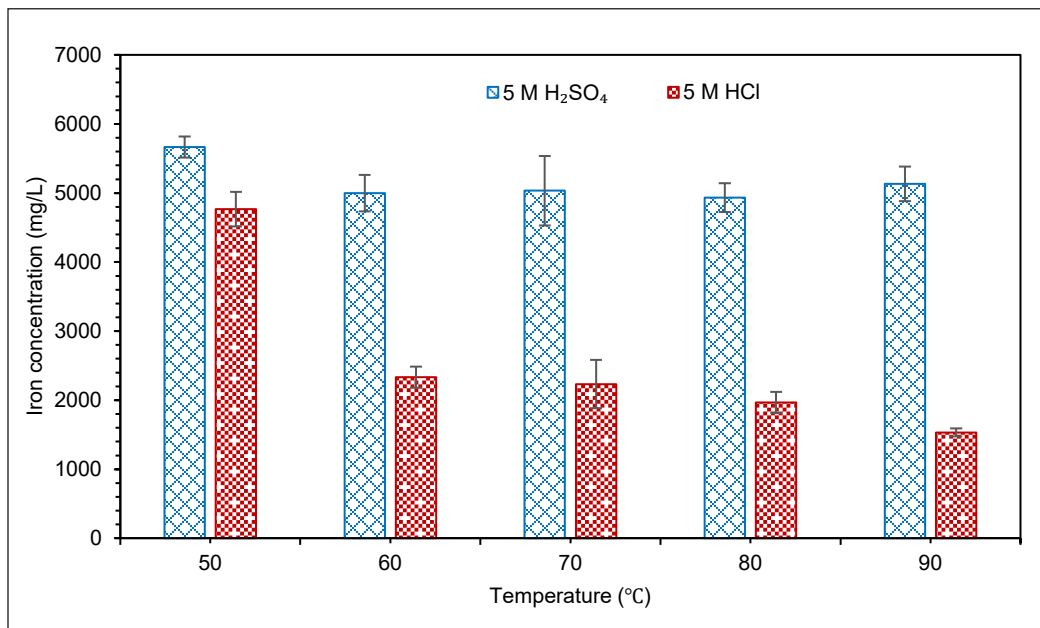

Figure 1. Effect of temperature on iron concentration in leachate

Effect of Oxidant Concentration

The oxidant concentration varied between 0.5–2 M, and the result is depicted in Figures 2a and 2b. It can be seen that the difference in H_2O_2 oxidant concentration between 0.5 and 1 M increased the iron recovery. Li et al. (2021) reported that an increase in the amount of hydrogen peroxide could provide more O^{2-} but the leaching efficiency would slowly decrease when the concentration of H_2O_2 is increased to a certain extent. However, an overdose supply of H_2O_2 may cause radical quenching, which reduces oxidant utilisation efficiency, limiting iron dissolution (Wang et al., 2021). It can also be seen that the recovery of iron in HCl with H_2O_2 as the oxidant all took place at approximately 8000 mg/L, which indicates that the effect of H_2O_2 concentration was not significant. $KMnO_4$, on the other side, is capable of recovering more iron in HCl compared to H_2SO_4. The recovery of iron decreases after 1 M in H_2SO_4 and HCl because the iron was saturated at 8000 mg/L in the leaching solution (Linsong et al., 2020). Lie et al. (2021) reported that the equilibrium state happened since all acidity was consumed; hence, no more iron could be leached out. The oxidation potential of H_2O_2 was 18 V. Meanwhile, KMnO4 was 1.7 V. It was indicated that H_2O_2 is better than $KMnO_4$ even though the oxidation potential difference between each oxidant was not quite notable. H_2O_2 was known as a very reactive and the most powerful oxidiser. Thus, the optimum oxidant concentration was 1M H_2O_2 in H_2SO_4.
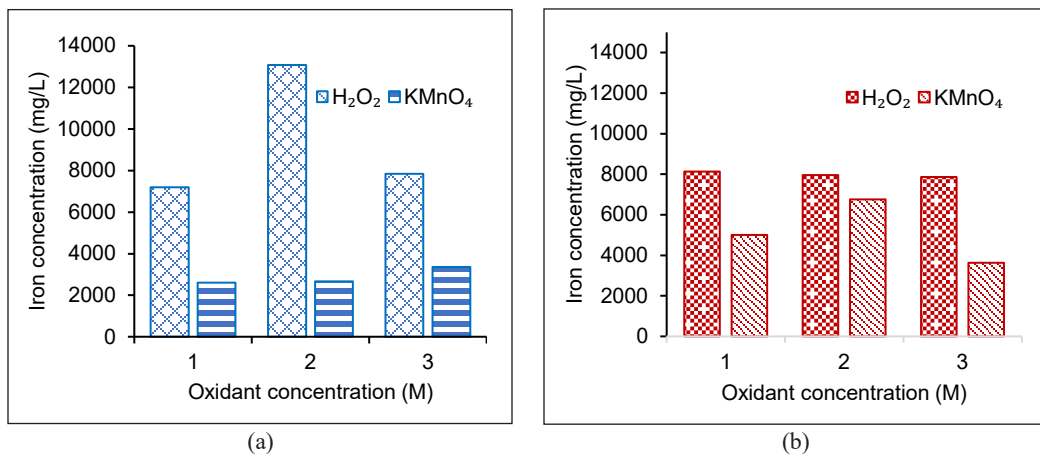

Figure 2. Amount of iron recovered at different H_2O_2 concentration and $KMnO_4$ concentrations in different leaching agents: (a) H_2SO_4; and (b) HCl
The function of H_2SO_4 and HCl were to serve as the oxidant that can help in increasing leaching efficiency

Effect of Acid Concentration

The effects of the concentration between 0.5-8 M were studied and are depicted in Figure 3. It can be seen that iron dissolution started between 0.5 M sulphuric acid and drastically increased at 1 M. The explanation for this is that the activity of the H^+ (protons) was

related to the reaction of the iron with the acid medium when the concentration of acid was increased (Hazaveh et al., 2020). However, the concentration of 8 M H_2SO_4 decreased iron leaching efficiency because of the formation of passive films that hindered further dissolution of the metal (Ichlas et al., 2020). The passive film appeared primarily composed of calcium oxide, resistant to sulphuric acid at high concentrations. Besides, the leaching was not solely controlled by the total metal content but was also significantly affected by other factors such as pH (Sun & Yi, 2021). The non-existing bar in 0.5 M H_2SO_4 denoted that no iron was leached out into the solution. When the HCl concentration was changed to between 1 and 3 M, the leaching efficiency of iron became more obvious with the increase of HCl concentration. Due to the volatilisation of HCl at high concentration, the leaching reaction has completed and remained steady as the concentrations were further raised to 8 M, with an average iron concentration of 7933 mg/L (Li et al., 2021). The metal ions tend to hydrolyse HCl ions quicker and inhibit HCl from being utilised effectively. In conclusion, 5 M was the most excellent acid concentration for recovering the most iron from EAFS.
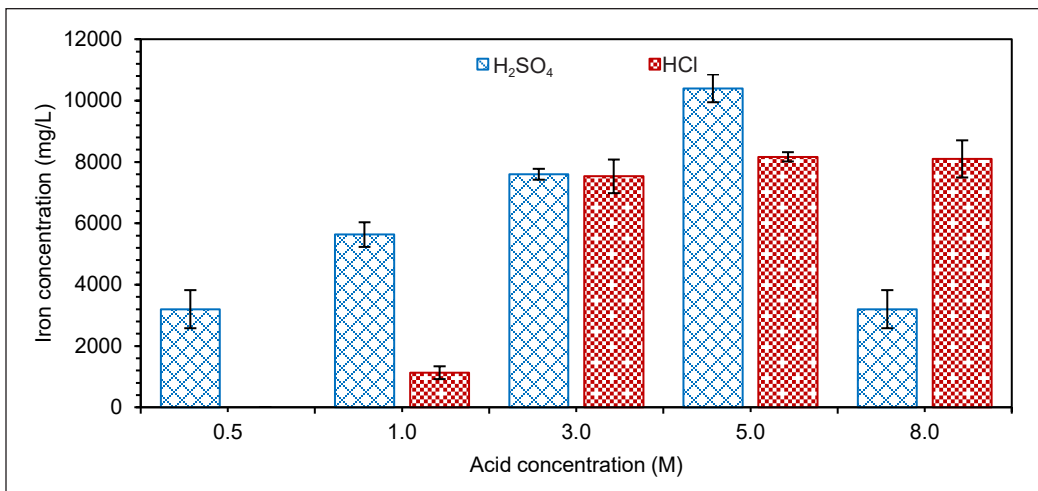

Figure 3. Effect of acid concentration on iron concentration after leaching

CONCLUSION

This study has focused on the leaching of electric arc furnace slag (EAFS) in the oxidative and non-oxidative leaching environment for the selective recovery of iron. In conclusion, the leaching performance was far better in a sulphuric acid environment than in hydrochloric acid. It can be concluded that the leaching efficiency of iron from EAFS can be further maximised in the appropriate conditions. Further study is necessary to analyse the iron-rich leached solution's kinetics and electrochemical activity.

ACKNOWLEDGMENT

REFERENCES

Brooks, L., Gaustad, G., Gesing, A., Mortvedt, T., & Freire, F. (2019). Ferrous and non-ferrous recycling: Challenges and potential technology solutions. *Waste Manag, 85*, 519-528. https://doi.org/10.1016/j. wasman.2018.12.043

Fisher, L. V., & Barron, A. R. (2019). The recycling and reuse of steelmaking slags - A review. *Resources, Conservation and Recycling, 146*, 244-255. https://doi.org/10.1016/j.resconrec.2019.03.010

Hafez, H., Kassim, D., Kurda, R., Silva, R. V., & de Brito, J. (2021). Assessing the sustainability potential of alkali-activated concrete from electric arc furnace slag using the ECO_2 framework. *Construction and Building Materials, 281*, Article 122559. https://doi.org/10.1016/j.conbuildmat.2021.122559

Halli, P., Agarwal, V., Partinen, J., & Lundström, M. (2020). Recovery of Pb and Zn from a citrate leach liquor of a roasted EAF dust using precipitation and solvent extraction. *Separation and Purification Technology, 236*, Article 116264. https://doi.org/10.1016/j.seppur.2019.116264

Hazaveh, P., Karimi, S., Rashchi, F., & Sheibani, S. (2020). Purification of the leaching solution of recycling zinc from the hazardous electric arc furnace dust through an as-bearing jarosite. *Ecotoxicology and Environmental Safety, 202*, Article 110893. https://doi.org/10.1016/j.ecoenv.2020.110893

Ichlas, Z. T., Rustandi, R. A., & Mubarok, M. Z. (2020). Selective nitric acid leaching for recycling of lead-bearing solder dross. *Journal of Cleaner Production, 264,* Article 121675. https://doi.org/10.1016/j. jclepro.2020.121675

Ji, H., Mi, X., Tian, Q., Liu, C., Yao, J., Ma, S., & Zeng, G. (2021). Recycling of mullite from high-alumina coal fly ash by a mechanochemical activation method: Effect of particle size and mechanism research. *Science of The Total Environment, 784*, Article 147100. https://doi.org/10.1016/j.scitotenv.2021.147100

Keymanesh, M. R., Ziari, H., Zalnezhad, H., & Zalnezhad, M. (2021). Mix design and performance evaluation of microsurfacing containing electric arc furnace (EAF) steel slag filler. *Construction and Building Materials, 269*, Article 121336. https://doi.org/10.1016/j.conbuildmat.2020.121336

Kim, J., & Azimi, G. (2020). Technospheric mining of niobium and titanium from electric arc furnace slag. *Hydrometallurgy, 191*, Article 105203. https://doi.org/10.1016/j.hydromet.2019.105203

Kremser, K., Thallner, S., Strbik, D., Spiess, S., Kucera, J., Vaculovic, T., Vsiansky, D., Haberbauer, M., Mandl, M., & Guebitz, G. M. (2021). Leachability of metals from waste incineration residues by iron- and sulfur-oxidizing bacteria. *Journal of Environmental Management, 280*, Article 111734. https://doi. org/10.1016/j.jenvman.2020.111734

Kukurugya, F., Vindt, T., & Havlík, T. (2015). Behavior of zinc, iron and calcium from electric arc furnace (EAF) dust in hydrometallurgical processing in sulfuric acid solutions: Thermodynamic and kinetic aspects. *Hydrometallurgy, 154*, 20-32. https://doi.org/10.1016/j.hydromet.2015.03.008

Li, P., Luo, S. H., Wang, Y., Yan, S., Teng, F., Feng, J., Wang, Q., Zhang, Y., Mu, Wenning., Zhai, X., & Liu, X. (2021). Cleaner and effective recovery of metals and synthetic lithium-ion batteries from extracted vanadium residue through selective leaching. *Journal of Power Sources, 482,* Article 228970. https://doi.org/10.1016/j.jpowsour.2020.228970

Lie, J., Lin, Y. C., & Liu, J. C. (2021). Process intensification for valuable metals leaching from spent NiMH batteries. *Chemical Engineering and Processing - Process Intensification, 167,* Article 108507. https://doi.org/10.1016/j.cep.2021.108507

Linsong, W., Peng, Z., Yu, F., Sujun, L., Yue, Y., Li, W., & Wei, S. (2020). Recovery of metals from jarosite of hydrometallurgical nickel production by thermal treatment and leaching. *Hydrometallurgy, 198,* Article 105493. https://doi.org/10.1016/j.hydromet.2020.105493

Martinho, F. C. G., Picado-Santos, L. G., & Capitão, S. D. (2018). Influence of recycled concrete and steel slag aggregates on warm-mix asphalt properties. *Construction and Building Materials, 185*, 684-696. https://doi.org/10.1016/j.conbuildmat.2018.07.041

Mohammadzadeh, M., Bagheri, H., & Ghader, S. (2020). Study on extraction and separation of Ni and Zn using [bmim][PF6] IL as selective extractant from nitric acid solution obtained from zinc plant residue leaching. *Arabian Journal of Chemistry, 13*(6), 5821-5831. https://doi.org/10.1016/j.arabjc.2020.04.019

Monosi, S., Ruello, M. L., & Sani, D. (2016). Electric arc furnace slag as natural aggregate replacement in concrete production. *Cement and Concrete Composites, 66*, 66-72. https://doi.org/10.1016/j.cemconcomp.2015.10.004

Nasuha, N., Ismail, S., & Hameed, B. H. (2016). Activated electric arc furnace slag as an efficient and reusable heterogeneous Fenton-like catalyst for the degradation of Reactive Black 5. *Journal of the Taiwan Institute of Chemical Engineers, 67*, 235-243. https://doi.org/10.1016/j.jtice.2016.07.023

Nasuha, N., Ismail, S., & Hameed, B. H. (2017). Activated electric arc furnace slag as an effective and reusable Fenton-like catalyst for the photodegradation of methylene blue and acid blue 29. *Journal of Environmental Management, 196*, 323-329. https://doi.org/10.1016/j.jenvman.2017.02.070

Nasuha N, Shaziela N, et al. (2019) Recovery of iron from electric arc furnace slag: effect of heating temperature and time. IOP Conference Series: Materials Science and Engineering 551. https://doi.org/10.1088/1757-899x/551/1/012119

Plaza, L., Castellote, M., Nevshupa, R., & Jimenez-Relinque, E. (2021). High-capacity adsorbents from stainless steel slag for the control of dye pollutants in water. *Environmental Science and Pollution Research, 28*, 23896-23910. https://doi.org/10.1007/s11356-020-12174-0

Rao, M., Shahin, C., & Jha, R. (2021). Optimization of leaching of copper to enhance the recovery of gold from liberated metallic layers of WPCBs. *Materials Today: Proceedings, 46*(3), 1515-1518. https://doi.org/10.1016/j.matpr.2021.01.052

Roy, S., Miura, T., Nakamura, H., & Yamamoto, Y. (2018). Investigation on applicability of spherical shaped EAF slag fine aggregate in pavement concrete - Fundamental and durability properties. *Construction and Building Materials, 192*, 555-568. https://doi.org/10.1016/j.conbuildmat.2018.10.157

Roy, S., Miura, T., Nakamura, H., & Yamamoto, Y. (2019). Investigation on material stability of spherical shaped EAF slag fine aggregate concrete for pavement during thermal change. *Construction and Building Materials, 215*, 862-874. https://doi.org/10.1016/j.conbuildmat.2019.04.228

Roy, S., Miura, T., Nakamura, H., & Yamamoto, Y. (2020). High temperature influence on concrete produced by spherical shaped EAF slag fine aggregate - Physical and mechanical properties. *Construction and Building Materials, 231,* Article 117153. https://doi.org/10.1016/j.conbuildmat.2019.117153

Sun, X., & Yi, Y. (2021). Acid washing of incineration bottom ash of municipal solid waste: Effects of pH on removal and leaching of heavy metals. *Waste Management, 120*, 183-192. https://doi.org/10.1016/j.wasman.2020.11.030

Teo, P. T., Anasyida, A. S., Kho, C. M., & Nurulakmal, M. S. (2019). Recycling of Malaysia's EAF steel slag waste as novel fluxing agent in green ceramic tile production: Sintering mechanism and leaching assessment. *Journal of Cleaner Production, 241,* Article 118144. https://doi.org/10.1016/j.jclepro.2019.118144

Wang, F., Gu, Z., Hu, Y., & Li, Q. (2021). Split dosing of H_2O_2 for enhancing recalcitrant organics removal from landfill leachate in the $Fe0/H_2O_2$ process: Degradation efficiency and mechanism. *Separation and Purification Technology, 278,* Article 119564. https://doi.org/10.1016/j.seppur.2021.119564

Yang, G. C. C., Chuang, T. N., & Huang, C. W. (2017). Achieving zero waste of municipal incinerator fly ash by melting in electric arc furnaces while steelmaking. *Waste Management, 62*, 160-168. https://doi.org/10.1016/j.wasman.2017.02.021

Yin, W., & Chen, K. (2021). Effect of the particle size and microstructure characteristics of the sample from HPGR on column bioleaching of agglomerated copper ore. *Hydrometallurgy, 200,* Article 105563. https://doi.org/10.1016/j.hydromet.2021.105563

Zhang, N., Wu, L., Liu, X., & Zhang, Y. (2019). Structural characteristics and cementitious behavior of basic oxygen furnace slag mud and electric arc furnace slag. *Construction and Building Materials, 219*, 11-18. https://doi.org/10.1016/j.conbuildmat.2019.05.156

Zhang, S., & Liu, W. (2017). Application of aerial image analysis for assessing particle size segregation in dump leaching. *Hydrometallurgy, 171*, 99-105. https://doi.org/10.1016/j.hydromet.2017.05.001